1 **Original Research Article**

2 **Title**

3 **Simultaneous changes in high-fat and high-cholesterol diet-induced**
4 **steatohepatitis and severe fibrosis and those underlying molecular mechanisms in**
5 **novel SHRSP5/Dmcr rat**

6 **Authors and Affiliations**

7 **Authors' names**

8 **Takashi Moriya · Kazuya Kitamori · Hisao Naito · Yukie Yanagiba · Yuki Ito ·**
9 **Nozomi Yamagishi · Hazuki Tamada · Xiaofang Jia · Satoru Tsuchikura ·**
10 **Katsumi Ikeda · Yukio Yamori · Tamie Nakajima**

11 Affiliations

12 T. Moriya · H. Naito · Y. Yanagiba · Y. Ito · N. Yamagishi · H. Tamada · X. Jia · T.
13 Nakajima (*)
14 Department of Occupational and Environmental Health,
15 Nagoya University Graduate School of Medicine,
16 65 Tsurumai-cho, Showa-ku, Nagoya 466-8550, Japan
17 * E-mail: tnasu23@med.nagoya-u.ac.jp

18 K. Kitamori · H. Tamada
19 Department of Food and Nutritional Environment,
20 Kinjo Gakuin University, Nagoya, Aichi, Japan

21 Y. Yanagiba
22 Mechanism of Health Effects Research Group,
23 National Institute of Occupational Safety and Health - Japan, Kawasaki, Kanagawa,
24 Japan

25

Y. Ito
Department of Occupational and Environmental Health,
Nagoya City University Graduate School of Medical Sciences, Nagoya, Aichi, Japan

S. Tsuchikura
Division of Breeding Management,
Disease Model Cooperative Research Association, Kyoto, Kyoto, Japan

K. Ikeda
School of Pharmacy and Pharmaceutical Sciences,
Mukogawa Women's University, Nishinomiya, Hyogo, Japan

Y. Yamori
Institute for World Health Development,
Mukogawa Women's University, Nishinomiya, Hyogo, Japan

Correspondence and request for materials
Dr. Tamie Nakajima
Address:
Department of Occupational and Environmental Health,
Nagoya University Graduate School of Medicine,
65 Tsurumai-cho, Showa-ku,
Nagoya, 466-8550
JAPAN
Tel: +81-52-744-2122
Fax: +81-52-744-2126
E-mail: tnasu23@med.nagoya-u.ac.jp

Keywords
Steatohepatitis · Inflammation · TNF-α · NF-κB · Fibrosis

Abbreviations:

HFC-diet	High fat and cholesterol-containing diet
SHRSP5/Dmcr	Stroke-prone, spontaneously hypertensive 5/Dmcr rat
TNF-α	Tumor necrosis factor-α
TGF-β1	Transforming growth factor-β1
PDGF-B	Platelet-derived growth factor-B
α-SMA	α-smooth muscle actin
NASH	Nonalcoholic steatohepatitis
NAFLD	Nonalcoholic fatty liver disease
MCD diet	Methionine and choline-deficient diet
PPARα	Peroxisome proliferator-activated receptor α
SP-diet	Stroke-prone control chow
H.E.	Hematoxylin and eosin
AST	Aspartate amonitransferase
ALT	Alanine aminotransferase
ELISA	Enzyme-linked immunosorbent assay
AdipoR1	Adiponectin receptor 1
AdipoR2	Adiponectin receptor 2
GAPDH	Glyceraldehydes-3-phosphate dehydrogenase
NF-κB	Nuclear factor-κB
IκBα	Inhibitor of κBα
SOD1	Cu^{2+}/Zn^{2+}-superoxide dismutase
AMPKα1/2	5'-adenosine monophosphate (AMP)-activated protein kinase α
subunit 1/2	
p-AMPKα	Phosphorylated AMPKα
PPARγ	Peroxisome proliferator-activated receptor γ
PH	Peroxisomal bifunctional protein (hydratase+3-hydroxyacyl-CoA
dehydrogenase)	
MCAD	Medium chain acyl-CoA dehydrogenase
DGAT1	Diacylglycerol acyltransferase 1
DGAT2	Diacylglycerol acyltransferase 2
HSC	Hepatic stellate cells

Abstract

Objectives This study aimed to show the molecular mechanisms underlying high-fat and high-cholesterol (HFC) diet-induced steatohepatitis and associated liver fibrosis progression in a novel stroke-prone, spontaneously hypertensive 5/Dmcr (SHRSP5/Dmcr) rat model.

Methods SHRSP5/Dmcr rats were treated with the control or HFC-diet for 2, 8, and 16 weeks. Plasma and hepatic gene expressions of key molecules involved in fatty acid oxidation, inflammation, oxidative stress and fibrosis were analyzed.

Results The HFC-diet increased plasma tumor necrosis factor-α (TNF-α) and hepatic p50/p65 signals, but reduced hepatic Cu^{2+}/Zn^{2+}-superoxide dismutase across the treatment period and plasma total adiponectin at 8 weeks. While transforming growth factor-β1 (TGF-β1) was elevated before obvious liver fibrosis pathology appeared at 2 weeks, the HFC-diet-induced platelet-derived growth factor-B (PDGF-B) and α-smooth muscle actin (α-SMA) corresponding to evident liver fibrosis at 8 weeks was followed by α_1 type I collagen production at 16 weeks. The HFC-diet increased hepatic total cholesterol accumulation although hepatic triglyceride declined by 0.3-fold from 2 to 16 weeks due to reduced hepatic triglyceride synthesis, as suggested by diacylglycerol acyltransferase 1 and 2.

104 *Conclusions* TNF-α and p50/p65 molecular signals appeared to be major factors for
105 HFC-diet-induced hepatic inflammation and oxidative stress facilitating liver disease
106 progression. While TGF-β1 being up-regulated before any evident liver fibrosis
107 appeared could be an early signal for progressive liver fibrosis, PDGF-B and α-SMA
108 signified evident liver fibrosis at 8 weeks followed by increased α_1 type I collagen
109 production and reduced triglyceride synthesis underlying extensive liver fibrosis at 16
110 weeks in novel SHRSP5/Dmcr model.
111

Introduction

Patients with fatty liver, nonalcoholic steatohepatitis (NASH), and associated fibrosis and cirrhosis, generically called nonalcoholic fatty liver disease (NAFLD), are increasing worldwide due to excess fat intake coupled with less physical activity in modern-day lifestyle [1-4]. While all stages of NAFLD, including NASH and associated liver fibrosis, have in common the fat infiltration of hepatocytes, the biochemical mechanisms behind the disease progression in humans have not been fully established [2]. Those are constrained by ethical issues with respect to repeated liver biopsies and by a limited ability to delineate cause-and-effect from complex interactive metabolic disease pathogeneses. This makes it difficult to distinguish NASH within NAFLD patients simply by clinical laboratory assessment [4, 5].

While various animal models with genetic, chemically-induced (e.g., carbon tetrachloride), or dietary (e.g., methionine and choline-deficient (MCD) diet) alterations show progression to the inflammatory condition of NASH [5], only a few rodent models appear to mimic the NASH pathology and the over-nutritional metabolic abnormality contexts of disease progression relevant to patients with liver diseases [5, 6]. In addition, many animal studies only characterize a limited experimental condition without sequentially following a time-course of liver disease

progression in detail. Indeed, these problems are partly due to the lack of good animal models with dietary-induced NASH and associated liver fibrosis, allowing a time-course evaluation of liver disease progression within a practically short period.

We have reported the stroke-prone spontaneously hypertensive 5/Dmcr rat (SHRSP5/Dmcr) strain, historically called arteriolipidosis-prone rats. They are registered at the National BioResource Project for the Rat in Japan [7], and are the 5th substrain of original SHRSP rat descended from the normotensive Wistar-Kyoto rat in Japan [8]. We have incidentally found extensive enlargement and whitish color of the fibrotic liver with extensive lipid accumulation in the SHRSP5/Dmcr [8] when we were investigating the effects of a high-fat and high-cholesterol containing (HFC) diet on arteriosclerosis rats in a nutritional research. The HFC-diet-induced steatohepatitis and liver fibrosis in the SHRSP5/Dmcr reflected pathological features closely resembling the steatohepatitis and liver fibrosis progression in patients despite no apparent hyperglycemia, insulin resistance and obesity [8]. From those pathological findings, perturbed lipid metabolism and increased inflammatory and pro-fibrogenic reactions from the HFC-diet were expected.

This initial study focused on revealing how a few key underlying molecular mechanisms, particularly genes associated with peroxisome proliferator-activated

148 receptor α (PPARα), tumor necrosis factor-α (TNF-α), transforming growth factor-β1
149 (TGF-β1), and platelet-derived growth factor-B (PDGF-B), would change at each stage
150 of liver disease progression, as bland steatosis advanced through progressive
151 inflammatory, oxidative stress, and fibrotic conditions, in this newly recognized
152 SHRSP5/Dmcr model. We found rather dynamic interplays and simultaneous changes
153 in the state of liver biochemical balance and the roles played by each gene associated
154 with hepatic inflammation, fibrosis, and fatty acid oxidation in novel SHRSP5/Dmcr
155 model.
156

Materials and methods

Animals

This animal study was approved by the Committee of Animal Experimentation (Approval No. 10) and conducted at Kinjo Gakuin University in accordance with its Animal Experiment Guidelines [8]. We obtained 30 male rat offspring at the age of 10 weeks that were used throughout our experiment by mating and housing, as described elsewhere [8]. They were provided with stroke-prone control chow (SP-diet) (Funabashi Farm, Chiba, Japan) [9] and water *ad libitum*. The nutrient components (weight %) of the SP-diet and the HFC-diet were described earlier [8]. At 10 weeks of age, 30 male rats were randomized to 6 groups: 3 groups were fed SP-diet (control), and the remaining groups were fed HFC-diet for 2, 8, and 16 weeks, respectively. During feeding, 2 out of 5 rats in the HFC-diet group died at 16 weeks (n = 3) due possibly to spontaneous stroke of SHRSP5/Dmcr rats [7]. At each time point, blood was collected from the abdominal aorta via syringe under pentobarbital anesthesia and directed into chilled tubes, and plasma was separated by centrifugation at 3000 rpm for 10 minutes. Then, all animals in each group were sacrificed under pentobarbital anesthesia, and the livers were quickly removed and weighed. A small liver section

174 was fixed in 4% buffered paraformaldehyde. The remaining liver and the plasma were

175 stored at -80°C until use [8].

176

177 Biochemical measurements in plasma and liver

178 Plasma aspartate amonitransferase (AST) and alanine aminotransferase (ALT)
179 activities were measured by the colorimetric method using a Transaminase C II Test
180 Kit (Wako Pure Chemical Industries, Osaka, Japan). Plasma triglyceride and total
181 cholesterol were quantified by TG E and TC E WAKO Kit, and liver triglyceride and
182 total cholesterol concentrations were obtained from aliquots of lipid extracts prepared
183 by the Folch method [10]. Furthermore, plasma total adiponectin concentration was
184 determined by an enzyme-linked immunosorbent assay (ELISA) kit (Otsuka
185 Pharmaceutical, Tokyo, Japan). Similarly, plasma TNF-α concentrations were
186 quantitatively measured by Quantikine® ELISA kit (R&D Systems, Minneapolis, MN,
187 USA).

188
189

190 Preparation of liver homogenate and nuclear fraction

191 Sections of whole rat liver samples were homogenized with three-fold (vol/wt) 10
192 mM phosphate buffer (pH 7.4) containing 0.25 M sucrose. Nuclear fraction from the
193 frozen liver of each rat was prepared using a CelLyticTM NuCLEARTM Extraction
194 Kit (SIGMA, Tokyo, Japan). Protein concentrations of the whole liver homogenate and

195 nuclear fraction were measured using Bio-Rad Protein Assay (Bio-Rad Laboratories,
196 Tokyo, Japan) [11, 12].
197
198 Western blot analyses
199 Samples of whole liver homogenate were subjected to 10% or 12.5%
200 polyacrylamide gel electrophoresis as described elsewhere [11-14]. The primary
201 polyclonal antibodies against adiponectin receptor 1 (AdipoR1) and 2 (AdipoR2)
202 (Alpha Diagnostic International, San Antonio, TX, USA), or α-smooth muscle actin
203 (α-SMA) (Sigma Aldrich, St. Louis, MO, USA) were purchased from a source shown
204 herein. The band was analyzed by densitometry, using the Lane and Spot Analyzer
205 version 5.0 (ATTO Corporation, Tokyo, Japan). Proteins measured from whole liver
206 tissue homogenate or nuclear fraction were normalized by the
207 glyceraldehydes-3-phosphate dehydrogenase (GAPDH) or histone H1, respectively,
208 within the same gel preparation.
209 Quantitative real-time PCR
210 mRNA concentration monitoring, total RNA isolation and complementary DNA
211 synthesis, and PCR primer mixture and PCR amplification cycle steps, were performed
212 by methods described elsewhere [11]. Primers were designed by using Primer Express
213 software (Applied Biosystems, Foster City, CA, USA), based on the sequence of

214 accession and GI numbers shown in Supplemental Table 1. Each mRNA level was
215 normalized to the level of GAPDH mRNA expression in the same preparation [11, 12].
216
217 Statistical analysis
218 Results are expressed as a mean ratio value ± SD to show the variance of original
219 data. Wilcoxon rank-sum test with the two-sided exact-test [15, 16] was performed at
220 each time-point of 2, 8, and 16 weeks (Windows SAS software version 8.2, Cary, NC,
221 USA) in order to statistically and precisely test the difference between the means of
222 two diet treatments (SP- and HFC-diet) for plasma, Western blot and mRNA data with
223 a significance of $P < 0.05$.
224

225 **Results**

226 Body and liver weight

227 Body weight showed no statistically significant differences between the two diet
228 groups at each treatment period (Table 1). Liver weight and ratio of liver and body
229 weight did not change in the SP-diet group throughout the treatment period, whereas it
230 increased significantly across 2, 8, and 16 weeks in the HFC diet group.

231

232 Plasma and hepatic lipid levels and plasma aminotransferase activities

233 To evaluate a state of lipid accumulation and metabolism, we measured triglyceride
234 and total cholesterol content in plasma and liver tissue. The plasma triglyceride levels
235 at 8 and 16 weeks in the HFC-diet group were greater than those in the SP-diet group
236 over the treatment period. It was considerably elevated at 16 weeks (a 5.1-fold change
237 in the mean from the 2-week period), although the inter-individual variance
238 contributed largely at 16 weeks. Liver triglyceride content at 2 weeks in the HFC-diet
239 group was significantly greater, although it declined by 0.3-fold from 2 to 16 weeks.

240 Plasma total cholesterol in the HFC-diet group showed a significantly higher
241 concentration than the SP-diet group across the treatment period, with a 1.6-fold rise
242 from 2 to 16 weeks. Furthermore, hepatic total cholesterol content in the HFC-diet

group was significantly greater than those in the SP-diet group across the treatment period, exhibiting a 1.7-fold change from 2 to 16 weeks.

To evaluate a state of liver injuries, we measured typical clinical markers of plasma ALT and AST values. For plasma ALT, mean values in the HFC-diet group were significantly different from those of the SP-diet group throughout the treatment period, with a 3.6-fold change from 2 to 16 weeks over time. Similarly, for plasma AST, a statistically significant difference was observed at 16 weeks with a 3.6-fold change from 2 to 16 weeks.

TNF-α, nuclear factor-κB (NF-κB) and oxidative stress responses

In order to evaluate response of inflammatory cytokine and association with total adiponectin, we measured TNF-α in plasma and liver. First, plasma TNF-α values in the HFC-diet group showed a convex time-course profile with significantly greater values than the SP-diet group, and a pronounced peak at 8 weeks, which was a 4.1-fold change from the mean value of the HFC-diet group at 2 weeks. In addition, hepatic TNF-α protein expression did not show any statistically significant differences between the diet groups at each treatment period (data not shown) because it might be released to the blood circulation. On the other hand, hepatic TNF-α mRNA expression

261 in the HFC-diet group was significantly up-regulated at each treatment period (Fig.
262 1A), and exhibited an identical convex time-course profile to plasma TNF-α
263 concentration in the HFC-diet group.

264 Second, for evaluation of NF-κB inflammatory signals in liver, we analyzed p50,
265 p65 and the inhibitor of κBα (IκBα). Hepatic p50 protein and mRNA expression in the
266 HFC-diet group were significantly up-regulated across the treatment period relative to
267 the SP-diet group (Fig. 1B, 1C and 1D). Moreover, p65 protein expression in the
268 HFC-diet group showed a significant 1.6-fold up-regulation at 8 weeks (Fig. 1E) while
269 its mRNA expression also demonstrated significantly greater values (1.7-, 2.4- and
270 2.2-fold at each respective week) than the SP-diet group at 2 and 16 weeks (Fig. 1F).
271 Furthermore, IκBα protein expression in the HFC-diet group was significantly
272 up-regulated at 2 and 8 weeks and declined by 0.9-fold at 16 weeks (Fig. 1G). The
273 mRNA expression of IκBα in the HFC-diet group did not show a statistically
274 significant difference between the diet groups (Fig. 1H).

275 Lastly, for evaluation of hepatic oxidative stress in relation to PPARα expression
276 [17], Cu^{2+}/Zn^{2+}-superoxide dismutase (SOD1) protein expression for the HFC-diet
277 group was significantly down-regulated across 2, 8, and 16 weeks (Fig. 1I), and its
278 mRNA expression was also significantly reduced from 8 weeks over the 16-week

279 period (Fig. 1J). This suggested a decrease in anti-oxidative stress within the liver,

280 because SOD1 is known to catalyze the dismutation of superoxide radicals produced

281 from the biological oxidation process and environmental stresses [17].

282

283 Plasma adiponectin and hepatic adiponectin receptors and 5'-adenosine
284 monophosphate-activated protein kinase α (AMPKα) responses

285 To evaluate mechanistic association of adiponectin with liver diseases, in the early
286 phase of diet treatment at 2 weeks, the mean total adiponectin concentration in plasma
287 for the HFC-diet group was significant and 1.3-fold greater than that of the SP-diet
288 group. Conversely, total adiponectin concentration at 8 weeks in the HFC-diet group
289 was significantly reduced by 0.8-fold relative to the SP-diet group.

290 On the other hand, hepatic AdipoR1 protein expression detected in the HFC diet
291 group was 2.8-fold, 1.3-fold and 1.6-fold relative to the SP-diet group at each
292 respective week, with a 2.0-fold change from 2 to 16 weeks over the treatment period
293 (Fig. 2A and 2B). Similarly, hepatic AdipoR1 mRNA expression in the HFC-diet
294 group at 2 weeks was significantly higher than those in the SP-diet group (Fig. 2C).

295 AdipoR2 protein expression in the liver of the HFC-diet group showed a significant
296 increase at 8 and 16 weeks (Fig. 2D). This was contrary to hepatic AdipoR2 mRNA
297 expression in the HFC-diet group, which showed significantly lower expression than
298 the SP-diet group at 8 weeks (Fig. 2E). Hepatic AdipoR2 mRNA expression in the
299 HFC-diet group exhibited a 0.3-fold change from 2 to 16 weeks, which corresponded
300 to the 0.8-fold decrease in plasma total adiponectin concentration over time.

We further analyzed AMPKα subunit 1/2 (AMPKα1/2) and phosphorylated AMPKα (p-AMPKα) in the liver to further evaluate as a marker of energy metabolism associated with adiponectin and PPARα [20]. Hepatic protein expression in the HFC-diet group was significantly down-regulated at 16 weeks for AMPKα1/2 and p-AMPKα relative to the SP-diet group (Fig. 2F and 2G). This connoted a downstream decrease of various energy metabolism regulated by AMPKα [18-20].

PPARs and associated gene responses

As a primary regulator of peroxisomal, mitochondrial and microsomal fatty acid oxidation [21], hepatic PPARα protein expression in the HFC-diet group was induced by 1.3-fold at 2 weeks and was significantly up-regulated at 8 weeks, but suppressed at 16 weeks compared with the SP-diet group (Fig. 3A and 3B). Hepatic PPARα mRNA expression in the HFC-diet group was significantly up-regulated at 2 weeks, followed by an earlier significant down-regulation at 8 and 16 weeks (Fig. 3C) relative to its own protein expression after 2 weeks, while the SP-diet group exhibited almost the same constant protein and mRNA expressions across the treatment period. Similarly, as an indicator of hepatic lipid metabolism and fibrosis by stellate cells, peroxisome proliferator-activated receptor γ (PPARγ) protein expression in the HFC-diet group

319 was induced by 1.5-fold at 2 weeks and was significantly up-regulated at 8 weeks,
320 whereas it was suppressed by 0.5-fold at 16 weeks compared with the SP-diet group
321 (Fig. 3D). PPARγ mRNA expression in the HFC-diet group was induced by 3.8-fold at
322 2 weeks followed by a large reduction at 8 and 16 weeks (Fig. 3E).
323 To confirm changes in down-stream target of PPARα transcription, protein
324 expression of peroxisomal bifunctional protein (hydratase+3-hydroxyacyl-CoA
325 dehydrogenase) (PH) in the HFC-diet group was elevated 1.4-fold at 2 weeks and
326 declined significantly at 16 weeks (Fig. 3F), while its mRNA expression also increased
327 significantly by 3.5-fold at 2 weeks followed by a significantly large reduction at 16
328 weeks (Fig. 3G). Medium chain acyl-CoA dehydrogenase (MCAD) protein expression
329 in the HFC-diet group was significantly suppressed over 8 to 16 weeks (Fig. 3H),
330 while mRNA expression was elevated 1.7-fold at 2 weeks, followed by a significant
331 reduction at 8 and 16 weeks, when compared with the SP-diet group (Fig. 3I).
332 As a marker of triglyceride synthesis in liver, hepatic mRNA expression of
333 diacylglycerol acyltransferase 1 (DGAT1) and 2 (DGAT2) in the HFC group was
334 significantly down-regulated at 8 and 16 weeks (Fig. 3J and 3K), suggesting an
335 inhibition of triglyceride synthesis in liver [22-24].
336

337 Fibrosis-associated gene responses

338 We studied how well liver fibrogenesis (TGF-β1, PDGF-B and α-SMA) and
339 cellular matrix molecular markers (α_1 type I collagen) associated with our prior
340 pathological observations [8]. With regard to TGF-β1, both hepatic proteins at 2 and
341 16 weeks, and mRNA expression at each respective week in the HFC-diet group were
342 significantly greater than those of the SP-diet group over time (Fig. 4A, 4B and 4C).
343 PDGF-B also showed a similar significant profile for both protein and mRNA
344 expression at 8 and 16 weeks, respectively, although those expressions at 2 weeks were
345 2.3- and 2.5-fold, respectively (Fig. 4D and 4E). Furthermore, significant up-regulation
346 of hepatic α-SMA protein at 8 weeks and mRNA expression at 16 weeks in the
347 HFC-diet group became evident from the 8-week period over 16 weeks, compared to
348 the SP-diet group (Fig. 4F and 4G). Similar time-course profiles were observed for the
349 significant increase in α_1 type I collagen protein expression at 16 weeks, as well as its
350 mRNA expression at 8 and 16 weeks in the liver for the HFC-diet group (Fig. 4H and
351 4I).
352

353 **Discussion**

354 As we reported earlier [8], the present SHRSP5/Dmcr model under the HFC-diet
355 treatment for 16 weeks demonstrated a transition from steatosis, inflammation with
356 hepatocyte injury or ballooning, and a distinctive pattern of perivenular or pericellular
357 liver fibrosis that resembled key features observed in NASH and liver fibrosis patients
358 [1, 5, 25]. At a molecular level, unlike the contemporary notion of step-wise two- or
359 multiple-hit hypothesis [26, 27], we observed rather dynamic interplays and
360 simultaneous changes in the state of liver biochemical balances with TNF-α and
361 p50/p65 hepatic inflammatory reactions, in conjunction with pro-fibrogenic TGF-β1
362 responses that led to shift the liver disease progression to extensive liver fibrosis
363 underlaid by PDGF-B, α-SMA and α_1 type I collagen up-regulation, by PPARα, PH,
364 MCAD, AMPKα1/2 and p-AMPKα protein eventual down-regulation, and by DGAT1
365 and DGAT2 mRNA down-regulation.

366 Increased TNF-α gene expression and oxidative stress in the liver has been
367 observed in NASH patients [1, 28, 29] and other rodent models [6, 30-32], as well as
368 more advanced liver fibrosis accompanied by extensive hepatic TNF-α expression in
369 advanced NASH patients [1, 28]. We found the HFC-diet treatment appeared to
370 facilitate TNF-α-induced inflammatory reactions throughout the experimental period

371 with a pronounced peak at 8 weeks. Furthermore, significant up-regulation in hepatic
372 p50 and p65 protein in the HFC-diet group at 8 weeks implied liver inflammation
373 induced by NF-κB, the p50/p65 heterodimer [33, 34]. This elevation in p50 and p65
374 protein might be due to the reduced anti-inflammatory functions of PPARα [21, 35-37],
375 since the induction PPARα protein at 8 weeks did not activate its target genes of PH
376 and MCAD during the same 8-week treatment period. This elevation in p50 and p65
377 protein in the HFC-diet group could also be explained by continuous inflammatory
378 reactions of TNF-α, because NF-κB is located downstream of the TNF-α signal
379 pathways and activated by TNF-α [21, 33]. Similarly, evident down-regulation of
380 SOD1 protein in the HFC-diet group across the treatment period was observed despite
381 the induction of PPARα protein at 8 weeks, regulating SOD1 for anti-oxidative effects
382 in liver [17, 21, 38]. This reduced abundance of SOD1 protein appeared to be driven
383 primarily by TNF-α liver inflammation and partially by PPARα-induced fatty acid
384 oxidation generating cytotoxic reactive molecules, facilitating a decrease in
385 concentration of anti-oxidant enzymes in liver [21, 32]. Moreover, a decline in plasma
386 total adiponectin at 8 weeks inversely corresponded to the peak in plasma TNF-α,
387 antagonizing anti-inflammatory effects of adiponectin [6, 39-41] and further
388 supporting the presence of TNF-α-induced hepatic inflammation. Taken together with

389 increased plasma ALT and AST levels and aggravated liver pathological features [8],
390 the hepatic inflammation and cell injury induced by TNF-α at 2 weeks were rather
391 mild, but facilitated oxidative stress. In addition, TNF-α and NF-κB-dependent
392 inflammation and the superimposed oxidative stress became evident at 8 weeks,
393 facilitating the progression of steatosis to steatohepatitis and extensive liver fibrosis
394 after the 8-week treatment period in this SHRSP5/Dmcr model.

395 For fibrosis molecular markers, TGF-β1 in the HFC-diet group was clearly
396 up-regulated at 2 weeks without any presence of fibrosis features observed in the liver
397 pathology of our prior report [8]. While TGF-β1 is a cytokine known to facilitate
398 pro-fibrogenic reactions and liver fibrosis via hepatic stellate cells (HSC) activation
399 [25, 42, 43], this initial increase at 2 weeks might be triggered by the dietary cholate
400 contained in the HFC-diet stimulating the expressions of TGF-β1, α-SMA, and
401 collagen genes [44], in parallel with hepatic Kupffer cell or HSC sensitization
402 generating TGF-β1 in response to hepatic inflammation and cell injury [25, 42, 43].
403 However, α-SMA and α_1 type I collagen were not induced at 2 weeks, thereby
404 precluding a possibility of dietary effect by cholate in the HFC-diet at 2 weeks. Thus,
405 initial TGF-β1 activation at 2 weeks in association with TNF-α induction in liver might
406 be a good early signal for progressive liver fibrosis, at least in current SHRSP5/Dmcr

model. Following early TGF-β1 sensitization, the significant up-regulation of PDGF-B and α-SMA protein expressions in the HFC-diet group at 8 weeks, indicating the extensive activation of HSC in the HFC-diet group at 8 weeks [42, 43, 45], clearly corresponded to the initial appearance of liver fibrosis in our prior pathology results at the same treatment period [8]. With diminishing hepatic anti-oxidant enzymes as well as increasing hepatic inflammation after 8 weeks, the significant up-regulation of hepatic α_1 type I collagen protein with continuing effects of TGF-β1 and PDGF-B at 16 weeks suggested that the fundamental shifts in the extracellular matrix composition and collagen production for wound healing from liver cell injury [42] underlaid the progression to extensive liver fibrosis at the 16-week treatment period.

Circulating adiponectin is generally antagonized by TNF-α [6, 39-41], but we observed increased plasma total adiponectin and TNF-α in the HFC-diet group in the same 2-week treatment period that was consistently observed in our earlier report [8]. This increased plasma total adiponectin at 2 weeks might possibly be related to PPARγ, since mouse without liver-specific PPARγ-gene has shown decreased serum adiponectin levels [46], indicating a role for hepatic PPARγ in adiponectin regulations. However, based on our results of plasma total adiponectin and TNF-α, and hepatic PPARγ at 8 weeks, the significant hepatic PPARγ protein induction did not lead to

425 plasma total adiponectin elevation. Instead, the antagonizing effect of TNF-α against
426 adiponectin appeared to be greater. Furthermore, with the reduction of plasma total
427 adiponectin in the HCF-diet group at 8 weeks, we expected a corresponding reduction
428 of hepatic AdipoR1/R2 and downstream AMPKα1/2, and PPARα pathways based on
429 recently proposed molecular signal transduction cascade considered to be important for
430 the energy metabolism and fatty acid oxidation in liver [20, 47]. However, our results,
431 particularly those hepatic protein expressions, did not support links with the proposed
432 molecular signaling pathways. Hepatic AdipoR2, which is predominantly expressed in
433 the liver [20], showed rather increased protein expressions in the HFC-diet group
434 corresponding to the aggravation of liver fibrosis pathology at 8 and 16 weeks in our
435 prior report [8]. Hence, further research in both liver and adipose tissues is needed to
436 dissect adiponectin regulatory mechanisms in the progressive liver fibrosis.
437 A net retention of lipids within hepatocytes, mostly in the form of triglycerides, is a
438 prerequisite for the development of NASH and NAFLD in patients [2]. In the present
439 results, hepatic triglyceride contents in the HFC-diet group initially increased and
440 declined after 8 weeks, whereas hepatic total cholesterol kept accumulating with
441 increased liver weight and progressive liver pathological features [8]. We also
442 observed a sharp rise in plasma triglyceride from 8 to 16 weeks in the HFC-diet group,

443 which may be a reflection of hepatocyte necrosis and liver disease progression since
444 increased levels of circulating blood triglyceride (hypertriglyceridemia) are a feature of
445 human NASH patients [2, 29]. In addition, despite a collapse in homeostatic fatty acid
446 oxidation and energy metabolism functions by diminishing PPARα, PH, MCAD,
447 AMPKα1/2, and p-AMPKα proteins [20, 48, 49], hepatic triglyceride in the HFC-diet
448 group did not accumulate at 16 weeks. One explanation might lay in the other study
449 where the inhibition of triglyceride synthesis by DGAT2 inhibitor did not prevent
450 fibrosis in the MCD-diet fed mouse [24]. Their study suggested triglyceride itself
451 might not be hepatotoxic and have a role in preventing progressive liver damages [24].
452 We actually observed clear down-regulation of DGAT1 and DGAT2 mRNA
453 expressions in the HFC-diet group at 8 and 16 weeks. Hence, from a perspective of
454 lipid metabolism, it appeared that the decline in hepatic triglyceride and its synthesis
455 might relate and aggravate the liver disease conditions so as to cause the extensive
456 liver fibrosis in the current SHRSP5/Dmcr model.

457 Our SHRSP5/Dmcr model with non-obese feature has some limitations when
458 compared with a common metabolic abnormality observed in NAFLD or NASH
459 patients, such as obesity [1, 2, 5], due possibly to an intrinsic trait of rats [5]. Our
460 SHRSP5/Dmcr in the HFC-diet group suggested that most lipids, especially total

461 cholesterol, accumulated in liver with increased liver weight, since we did not find any
462 extensive lipid accumulation in mesentery or visceral adipose tissue during rat
463 sacrifice. Moreover, unlike the fatty acid contents, our HFC-diet contained very high
464 cholesterol and relatively low carbohydrates compared with the daily dietary intake of
465 obese NASH patients [32, 50]. Hence, the biological investigation in a role of
466 cholesterol underlying steatohepatitis and liver fibrosis in the SHRSP5/Dmcr is
467 necessary, and it is indeed a subject of on-going study by our co-workers [Naito, et al.
468 in preparation]. Lastly, we lost 2 out of 5 rats in the HFC-diet group under the 16-week
469 treatment period due possibly to spontaneous stroke of SHRSP5/Dmcr rats [7], and the
470 14-week treatment period might therefore be optimal for the current SHRSP5/Dmcr
471 model [8]. Besides other limitations, considering non-obese, lean human population
472 affected by NASH and liver fibrosis [51-54], as well as patients with non-obese,
473 non-diabetic NASH patients consuming high amounts of cholesterol and saturated fatty
474 acid [50], our novel SHRSP5/Dmcr model may be suited for investigating the
475 time-course of disease mechanisms for those lean, non-diabetic patients with
476 steatohepatitis and associated liver fibrosis.

477 In conclusion, TNF-α and p50/p65 molecular signals appeared to be major factors
478 for the HFC-diet-induced hepatic inflammation and oxidative stress facilitating the

479 liver disease progression. While TGF-β1 up-regulation occurring before any evident
480 liver fibrosis appeared could be an early signal for progressive liver fibrosis, PDGF-B
481 and α-SMA signified evident liver fibrosis at 8 weeks, followed by increased α_1 type I
482 collagen production and reduced triglyceride synthesis underlying extensive liver
483 fibrosis at 16 weeks in our novel SHRSP5/Dmcr model.
484

Acknowledgments

This study was supported in part by a Grant-in-Aid for Scientific Research (B23390161) from the Japan Society for the Promotion of Science, and the Uehara Memorial Foundation in 2009. No additional external funding received for this study. The funders had no role in study design, data collection and analysis, decision to publish, or preparation of the manuscript.

Author contributions

KK, HN, YY, YI, NY, HT, XJ, ST, KI, and YY contributed to this work. KK, ST, KI, and YY provided the SHRSP5/Dmcr rat strain, conducted animal experiments and analyzed liver samples. YY, YI and NY designed the primer for PCR analyses and supported the material procurement for various laboratory analyses. HN, YY, YI, XJ, and HT performed a part of plasma, Western blot and PCR analyses. TM performed the majority of the plasma, Western blot and PCR analyses, analyzed the data, and wrote the paper. TM, KK, HN, and TN contributed to the study design and interpretation of data.

Conflict of interest

All authors have declared that no conflict of interest exists.

503 **References**

504 1. Tilg H, Hotamisligil GS. Nonalcoholic fatty liver disease: Cytokine-adipokine
505 interplay and regulation of insulin resistance. Gastroenterology. 2006;131:934-45.

506 2. Angulo P. Nonalcoholic fatty liver disease. N Engl J Med. 2002;346:1221-31.

507 3. Hashimoto E, Tokushige K. Prevalence, gender, ethnic variations, and prognosis of
508 NASH. J Gastroenterol. 2011;46(Suppl 1):63-9.

509 4. Powell EE, Jonsson JR, Clouston AD. Dangerous liaisons: the metabolic syndrome
510 and nonalcoholic fatty liver disease. Ann Intern Med. 2005;143:753-54.

511 5. Larter CZ, Yeh MM. Animal models of NASH: getting both pathology and
512 metabolic context right. J Gastroenterol Hepatol. 2008;23:1635-48.

513 6. Svegliati-Baroni G, Candelaresi C, Saccomanno S, Ferretti G, Bachetti T, Marzioni
514 M, et al. A model of insulin resistance and nonalcoholic steatohepatitis in rats: role
515 of peroxisome proliferator-activated receptor-α and n-3 polyunsaturated fatty acid
516 treatment on liver injury. Am J Pathol. 2006;169:846-60.

517 7. Yamori Y. Selection of arteriolipidosis-prone rats (ALR). Jpn Heart J.
518 1977;18:602-3.

519 8. Kitamori K, Naito H, Tamada H, Kobayashi M, Miyazawa D, Yasui Y, et al.
520 Development of novel rat model for high-fat and high-cholesterol diet-induced
521 steatohepatitis and severe fibrosis progression in SHRSP5/Dmcr. Environ Health
522 Prev Med. 2011;[Epub ahead of print]:1-10.

523 9. Sansawa H, Takahashi M, Tsuchikura S, Endo H. Effect of chlorella and its
524 fractions on blood pressure, cerebral stroke lesions, and life-span in stroke-prone
525 spontaneously hypertensive rats. J Nutr Sci Vitaminol (Tokyo). 2006;52:457-66.

526 10. Folch J, Lees M, Sloane Stanley GH. A simple method for the isolation and
527 purification of total lipides from animal tissues. J Biol Chem. 1957;226:497-509.

528 11. Ito Y, Yamanoshita O, Asaeda N, Tagawa Y, Lee CH, Aoyama T, et al.
529 Di(2-ethylhexyl)phthalate induces hepatic tumorigenesis through a peroxisome

530 proliferator-activated receptor α-independent pathway. J Occup Health.
531 2007;49:172-82.

532 12. Ramdhan DH, Kamijima M, Yamada N, Ito Y, Yanagiba Y, Nakamura D, et al.
533 Molecular mechanism of trichloroethylene-induced hepatotoxicity mediated by
534 CYP2E1. Toxicol and Appl Pharmacol. 2008;231:300-7.

535 13. Aoyama T, Peters JM, Iritani N, Nakajima T, Furihata K, Hashimoto T, et al.
536 Altered constitutive expression of fatty acid-metabolizing enzymes in mice lacking
537 the peroxisome proliferator-activated receptor alpha (PPARα). J Biol Chem.
538 1998;273:5678-84.

539 14. Okiyama W, Tanaka N, Nakajima T, Tanaka E, Kiyosawa K, Gonzalez FJ, et al.
540 Polyenephosphatidylcholine prevents alcoholic liver disease in PPARα-null mice
541 through attenuation of increases in oxidative stress. J Hepatol. 2009;50:1236-46.

542 15. Wilcoxon F. Individual comparisons by ranking methods. Biometrics Bulletin.
543 1945;1:80-3.

544 16. Bauer DF. Constructing confidence sets using rank statistics. Journal of the
545 American Statistical Association. 1972;67:687-90.

546 17. Yoo HY, Chang MS, Rho HM. Induction of the rat Cu/Zn superoxide dismutase
547 gene through the peroxisome proliferator-responsive element by arachidonic acid.
548 Gene. 1999;234:87-91.

549 18. Ruderman N, Prentki M. AMP kinase and malonyl-CoA: targets for therapy of the
550 metabolic syndrome. Nat Rev Drug Discov. 2004;3:340-51.

551 19. Long YC, Zierath JR. AMP-activated protein kinase signaling in metabolic
552 regulation. J Clin Invest. 2006;116:1776-83.

553 20. Yamauchi T, Nio Y, Maki T, Kobayashi M, Takazawa T, Iwabu M, et al. Targeted
554 disruption of AdipoR1 and AdipoR2 causes abrogation of adiponectin binding and
555 metabolic actions. Nat Med. 2007;13:332-9.

21. Mandard S, Muller M, Kersten S. Peroxisome proliferator-activated receptor α target genes.
Cell Mol Life Sci. 2004;61:393-416.

22. Yamazaki T, Sasaki E, Kakinuma C, Yano T, Miura S, Ezaki O. Increased very low density lipoprotein secretion and gonadal fat mass in mice overexpressing liver DGAT1. J Biol Chem. 2005;280:21506-14.

23. Cases S, Stone SJ, Zhou P, Yen E, Tow B, Lardizabal KD, et al. Cloning of DGAT2, a second mammalian diacylglycerol acyltransferase, and related family members. J Biol Chem. 2001;276:38870-6.

24. Yamaguchi K, Yang L, McCall S, Huang J, Yu XX, Pandey SK, et al. Inhibiting triglyceride synthesis improves hepatic steatosis but exacerbates liver damage and fibrosis in obese mice with nonalcoholic steatohepatitis. Hepatology. 2007;45:1366-74.

25. Friedman SL. Hepatic stellate cells: protean, multifunctional, and enigmatic cells of the liver. Physiol Rev. 2008;88:125-72.

26. Day CP, James OF. Steatohepatitis: a tale of two "hits"? Gastroenterology. 1998;114:842-5.

27. Lewis JR, Mohanty SR. Nonalcoholic fatty liver disease: a review and update. Dig Dis Sci. 2010;55:560-78.

28. Crespo J, Cayon A, Fernandez-Gil P, Hernandez-Guerra M, Mayorga M, Dominguez-Diez A, et al. Gene expression of tumor necrosis factor alpha and TNF-receptors, p55 and p75, in nonalcoholic steatohepatitis patients. Hepatology. 2001;34:1158-63.

29. Farrell GC, Larter CZ. Nonalcoholic fatty liver disease: from steatosis to cirrhosis. Hepatology. 2006;43:S99-112.

30. Uysal KT, Wiesbrock SM, Marino MW, Hotamisligil GS. Protection from obesity-induced insulin resistance in mice lacking TNF-α function. Nature. 1997;389:610-4.

584 31. Fu JH, Xie SR, Kong SJ, Wang Y, Wei W, Shan Y, et al. The combination of a
585 high-fat diet and chronic stress aggravates insulin resistance in Wistar male rats.
586 Exp Clin Endocrinol Diabetes. 2009;117:354-60.

587 32. Romestaing C, Piquet MA, Bedu E, Rouleau V, Dautresme M, Hourmand-Ollivier
588 I, et al. Long term highly saturated fat diet does not induce NASH in Wistar rats.
589 Nutr Metab (Lond). 2007;4:4.

590 33. Plumpe J, Malek NP, Bock CT, Rakemann T, Manns MP, Trautwein C. NF-κB
591 determines between
592 apoptosis and proliferation in hepatocytes during liver regeneration. Am J Physiol
593 Gastrointest Liver Physiol. 2000;278:G173-83.

594 34. Chakraborty JB, Mann DA. NF-κB signalling: Embracing complexity to achieve
595 translation.
596 J of Hepatol. 2010;52:285-91.

597 35. Delerive P, De Bosscher K, Besnard S, Vanden Berghe W, Peters JM, Gonzalez FJ,
598 et al. Peroxisome proliferator-activated receptor α negatively regulates the vascular
599 inflammatory gene response by negative cross-talk with transcription factors
600 NF-κB and AP-1. J Biol Chem. 1999;274:32048-54.

601 36. Delerive P, Gervois P, Fruchart JC, Staels B. Induction of IκBα expression as a
602 mechanism
603 contributing to the anti-inflammatory activities of peroxisome
604 proliferator-activated receptor-α activators. J Biol Chem. 2000;275:36703-7.

605 37. Ricote M, Li AC, Willson TM, Kelly CJ, Glass CK. The peroxisome
606 proliferator-activated receptor-γ is a negative regulator of macrophage activation.
607 Nature. 1998;391:79-82.

608 38. Nakajima T, Kamijo Y, Tanaka N, Sugiyama E, Tanaka E, Kiyosawa K, et al.
609 Peroxisome proliferator-activated receptor α protects against alcohol-induced liver
610 damage. Hepatology. 2004;40:972-80.

611 39. Maeda N, Takahashi M, Funahashi T, Kihara S, Nishizawa H, Kishida K, et al.
612 PPARγ ligands increase expression and plasma concentrations of adiponectin, an
613 adipose-derived protein. Diabetes. 2001;50:2094-9.

614 40. Maeda N, Shimomura I, Kishida K, Nishizawa H, Matsuda M, Nagaretani H, et al.
615 Diet-induced insulin resistance in mice lacking adiponectin/ACRP30. Nat Med.
616 2002;8:731-7.

617 41. Hui JM, Hodge A, Farrell GC, Kench JG, Kriketos A, George J.. Beyond insulin
618 resistance in NASH: TNF-α or adiponectin? Hepatology. 2004;40:46-54.

619 42. Friedman SL. Molecular regulation of hepatic fibrosis, an integrated cellular
620 response to tissue injury. J Biol Chem. 2000;275:2247-50.

621 43. Friedman SL. Liver fibrosis - from bench to bedside. J Hepatol. 2003;38(Suppl
622 1):S38-53.

623 44. Vergnes L, Phan J, Strauss M, Tafuri S, Reue K. Cholesterol and cholate
624 components of an atherogenic diet induce distinct stages of hepatic inflammatory
625 gene expression. J Biol Chem. 2003;278:42774-84.

626 45. Breitkopf K, Roeyen C, Sawitza I, Wickert L, Floege J, Gressner AM. Expression
627 patterns of PDGF-A, -B, -C and -D and the PDGF-receptors α and β in activated
628 rat hepatic stellate cells (HSC). Cytokine. 2005;31:349-57.

629 46. Gavrilova O, Haluzik M, Matsusue K, Cutson JJ, Johnson L, Dietz KR, et al. Liver
630 peroxisome proliferator-activated receptor γ contributes to hepatic steatosis,
631 triglyceride clearance, and regulation of body fat mass. J Biol Chem.
632 2003;278:34268-76.

633 47. Yamauchi T, Kamon J, Minokoshi Y, Ito Y, Waki H, Uchida S, et al. Adiponectin
634 stimulates glucose utilization and fatty-acid oxidation by activating AMP-activated
635 protein kinase. Nat Med. 2002;8:1288-95.

636 48. Tomita K, Azuma T, Kitamura N, Nishida J, Tamiya G, Oka A, et al. Pioglitazone
637 prevents alcohol-induced fatty liver in rats through up-regulation of c-Met.
638 Gastroenterology. 2004;126:873-85.

639 49. Belfort R, Harrison SA, Brown K, Darland C, Finch J, Hardies J, et al. A
640 placebo-controlled trial of pioglitazone in subjects with nonalcoholic
641 steatohepatitis. N Engl J Med. 2006;355:2297-307.

642 50. Musso G, Gambino R, De Michieli F, Cassader M, Rizzetto M, Durazzo M, et al.
643 Dietary habits and their relations to insulin resistance and postprandial lipemia in
644 nonalcoholic steatohepatitis. Hepatology. 2003;37:909-16.

645 51. Wanless IR, Lentz JS. Fatty liver hepatitis (steatohepatitis) and obesity: an autopsy
646 study with analysis of risk factors. Hepatology. 1990;12:1106-10.

647 52. Silverman JF, O'Brien KF, Long S, Leggett N, Khazanie PG, Pories WJ, et al.
648 Liver pathology in morbidly obese patients with and without diabetes. Am J
649 Gastroenterol. 1990;85:1349-55.

650 53. Speliotes EK, Massaro JM, Hoffmann U, Vasan RS, Meigs JB, Sahani DV, et al.
651 Fatty liver is associated with dyslipidemia and dysglycemia independent of
652 visceral fat: the Framingham Heart Study. Hepatology. 2010;51:1979-87.

653 54. Chitturi S, Wong VW, Farrell G. Nonalcoholic fatty liver in Asia: Firmly
654 entrenched and rapidly gaining ground. J Gastroenterol Hepatol. 2011;26(Suppl
655 1):163-72.

656

657

658 **Tables**

659

660 **Table 1.** Effects of HFC-diet on body and liver weight, biochemical characteristics in
661 plasma and liver at each treatment period.

662

663

664 **Footnote for Table 1**

665 Data have a mean value ± SD per each group. * $p<0.05$; **, $p<0.01$; compared with the
666 SP-diet group within each diet treatment period.

667

668 **Supplemental Table 1.** List of primers used for quantitative real-time PCR.

669

Tables

Table 1. Effects of HFC-diet on body and liver weight, biochemical characteristics in plasma and liver at each treatment period.

Diet treatment group	**SP-diet group**			**HFC-diet group**		
Treatment period	**2 weeks**	**8 weeks**	**16 weeks**	**2 weeks**	**8 weeks**	**16 weeks**
Body and Liver weight:						
Body weight (g)	224 ± 17	256 ± 13	271 ± 20	200 ± 25	237 ± 15	260 ± 39
Liver weight (g)	6.4 ± 0.5	6.6 ± 0.3	7.0 ± 0.4	8.6 ± 0.7 **	23.1 ± 2.4 **	31.1 ± 2.6 **
Liver weight / Body weight ratio	0.03 ± 0.001	0.03 ± 0.001	0.03 ± 0.002	0.04 ± 0.005 **	0.10 ± 0.008 **	0.12 ± 0.009 **
Plasma measurements:						
Triglyceride (mg/dl)	53.9 ± 20.2	41.4 ± 7.1	72.6 ± 18.0	71.4 ± 22.9	59.1 ± 11.7 *	366.2 ± 276.6 *
Total cholesterol (mg/dl)	29.7 ± 7.4	45.1 ± 7.6	47.1 ± 12.6	135.3 ± 57.0 **	112.6 ± 20.6 **	213.0 ± 116.8 *
ALT (IU/l)	16.7 ± 1.4	15.5 ± 1.4	23.3 ± 4.5	28.7 ± 3.8 *	35.5 ± 3.5 **	103.4 ± 59.1 *
AST (IU/l)	58.2 ± 12.3	101.6 ± 11.6	103.2 ± 25.9	68.8 ± 10.4	138.5 ± 35.6	245.5 ± 117.4 *
Total adiponectin (μg/ml)	5.4 ± 1.0	5.8 ± 0.6	6.1 ± 0.9	7.1 ± 0.8 *	4.7 ± 0.4 *	5.7 ± 1.1
TNF-α (pg/ml)	1.7 ± 0.3	2.4 ± 0.6	2.5 ± 1.6	4.7 ± 1.9 *	19.1 ± 7.8 *	13.7 ± 1.0 *
Liver measurements:						
Triglyceride (mg/g liver)	13.4 ± 3.9	23.8 ± 18.2	17.2 ± 3.9	47.8 ± 5.7 **	31.8 ± 3.5	12.5 ± 4.3
Total cholesterol (mg/g liver)	2.3 ± 0.5	1.7 ± 0.5	1.6 ± 0.1	100.2 ± 6.6 **	170.0 ± 12.9 **	170.8 ± 24.6 *

Data have a mean value ± SD per each group. * $p<0.05$; ** $p<0.01$; compared with the SP-diet group within each diet treatment period.

Supplemental Table 1. List of primers used for quantitative real-time PCR.

Rodent genes	Accession number	GI number	Forward (5'–3')	Reverse (5'–3')
AdipoR1	NM_207587.1	46485455	CTACATGGCCACAGACCACCTAT	CTGTGTGGATGCGGAAGATG
AdipoR2	NM_001037979.1	83816890	CAACCTTGCTTCATCTACCTGATTG	AACATGTCCCACTGAGAGACGAT
PPARα	NM_013196.1	6981381	ATGGAGTCCACGCATGTGAAG	ACGCCAGCTTTAGCCGAAT
PPARγ	NM_013124.2	148747595	CGCTGATGCACTGCCTATGA	AGAGGTCCACAGAGCTGATTCC
PH	NM_133606.1	19424317	TGGGCTGTCACTATCGGATTG	AGAGCAACAGGAACTCCAACGA
MCAD	NM_016986.1	8392832	AAAGCCTTCACCGGATTCATC	CCGCTGACCCATGTTTAGTTC
SOD1	BC082800.1	52350648	GCAGGACCTCATTTTAATCCTCACT	GGTCTCCAACATGCCTCTCTTC
p50	XM_342346.1	34860606	GCACTATGGATTTCCTGCTTACG	GGGTGATGCCTGTGTTGGAT
p65	AF079314.1	3388148	TCTGCCGAGTAAACCGGAACT	CCGTGAAATACACCTCAATGTCTT
TNF-α	X66539.1	395369	GACCCTCACACTCAGATCATCTTCT	TGCTTGGTGGTTTGCTACGA
IκBα	XM_343065.3	109478176	GTGAGGATGAGGAGAGCTATGACA	AATGGACCACTCTGGCAGTAATG
TGF-β1	NM_021578.2	148747597	CAACAATTCCTGGCGTTACCTT	GACGTCAAAAGACAGCCACTCA
PDGF-B	NM_031524.1	158081746	ACCACTCCATCCGCTCCTTT	CTTTCCGACTCGACTCCAGAA
α-SMA	NM_031004.2	148298812	ATGGGCCAAAAGGACAGCTA	TGATGATGCCGTGTTCTATCG
α_1 type I Collagen	NM_053304.1	158711703	ATGCTTGATCTGTATCTGCCACAAT	ACTCGCCCTCCCGTTTTT
DGAT1	NM_053437	17865334	GGCGGTCCCCAACCAT	GCTCTGCCACAGCATTGAGA
DGAT2	NM_001012345	59891414	TGGCCTGCAGTGTCATCCT	GGGCGTGTTCCAGTCAAATG
GAPDH	BC096440.1	66396585	AGAACATCATCCCTGCATCCA	CCGTTCAGCTCTGGGATGAC

Figure Legends

Fig 1. Effects of HFC-diet treatment on hepatic TNF-α, p50/p65 (NF-κB), IκBα, SOD1 protein and mRNA expressions. (A) TNF-α mRNA expression ratio. (B) Western blot results of respective protein expressions in whole liver tissue homogenates or nuclear fractions. (C) Hepatic p50 protein and (D) mRNA expression ratio. (E) Hepatic p65 protein and (F) mRNA expression ratio. (G) Hepatic IκBα protein and (H) mRNA expression ratio. (I) Hepatic SOD1 protein and (J) mRNA expression ratio. Each histogram represents a mean ratio ± SD. * $p<0.05$; ** $p<0.01$; compared with the SP-diet group within each diet-treatment period.

Fig 2. Effects of HFC-diet treatment on hepatic AdipoR1, AdipoR2, AMPKα1/2 and p-AMPKα protein and mRNA expressions. (A) Western blot results of respective protein expressions in whole liver tissue homogenates. (B) Hepatic AdipoR1 protein and (C) mRNA expression ratio. (D) Hepatic AdipoR2 protein and (E) mRNA expression ratio. (F) AMPKα1/2 and (G) p-AMPKα protein expression ratio. Each histogram represents a mean ratio ± SD. * $p<0.05$; ** $p<0.01$; compared with the SP-diet group within each diet-treatment period.

Fig 3. Effects of HFC-diet treatment on hepatic PPARα, PPARγ, PH, MCAD, SOD1, DGAT1 and DGAT2 protein and mRNA expressions. (A) Western blot results of respective protein expressions in whole liver tissue homogenates or nuclear fractions. (B) Hepatic PPARα protein and (C) mRNA expression ratio. (D) Hepatic PPARγ protein and (E) mRNA expression ratio. Ratio of hepatic protein and mRNA expressions for PH (F and G), MCAD (H and I). (J) Hepatic DGAT1 and (K) DGAT2 mRNA expression ratio. Each histogram represents a mean ratio ± SD. * $p<0.05$; ** $p<0.01$; compared with the SP-diet group within each diet-treatment period.

Fig 4. Effects of HFC-diet treatment on hepatic TGF-β1, PDGF-B, α-SMA and α_1 type I collagen protein and mRNA expressions. (A) Western blot results of respective protein expressions in whole liver tissue homogenates. (B) Ratio of TGF-β1 protein and (C) mRNA expressions. (D) Ratio of PDGF-B protein and (E) mRNA expressions. (F) Ratios of α-SMA protein and (G) mRNA expressions. (H) Ratio of α_1 type I collagen protein and (I) mRNA expressions. Each histogram represents a mean ratio ± SD. * $p<0.05$; ** $p<0.01$; compared with the SP-diet group within each diet-treatment period.

Fig 5. Schematic model for time-course changes in hepatic gene expressions of key factors during steatohepatitis and fibrosis progression in SHRSP5/Dmcr rat under HFC-diet treatment. Current SHRSP5/Dmcr rat model appeared to show rather dynamic interplays and changes in the state of liver biochemical balances with initial TNF-α and p50/p65 (NF-κB) hepatic inflammatory reactions, in conjunction with pro-fibrogenic TGF-β1 responses that led to shift the liver disease progression to extensive liver fibrosis underlaid by PDGF-B, α-SMA and α_1 type I collagen up-regulation, by PPARs and AMPKα associated proteins' eventual down-regulation, and by DGAT1 and DGAT2 mRNA down-regulation.

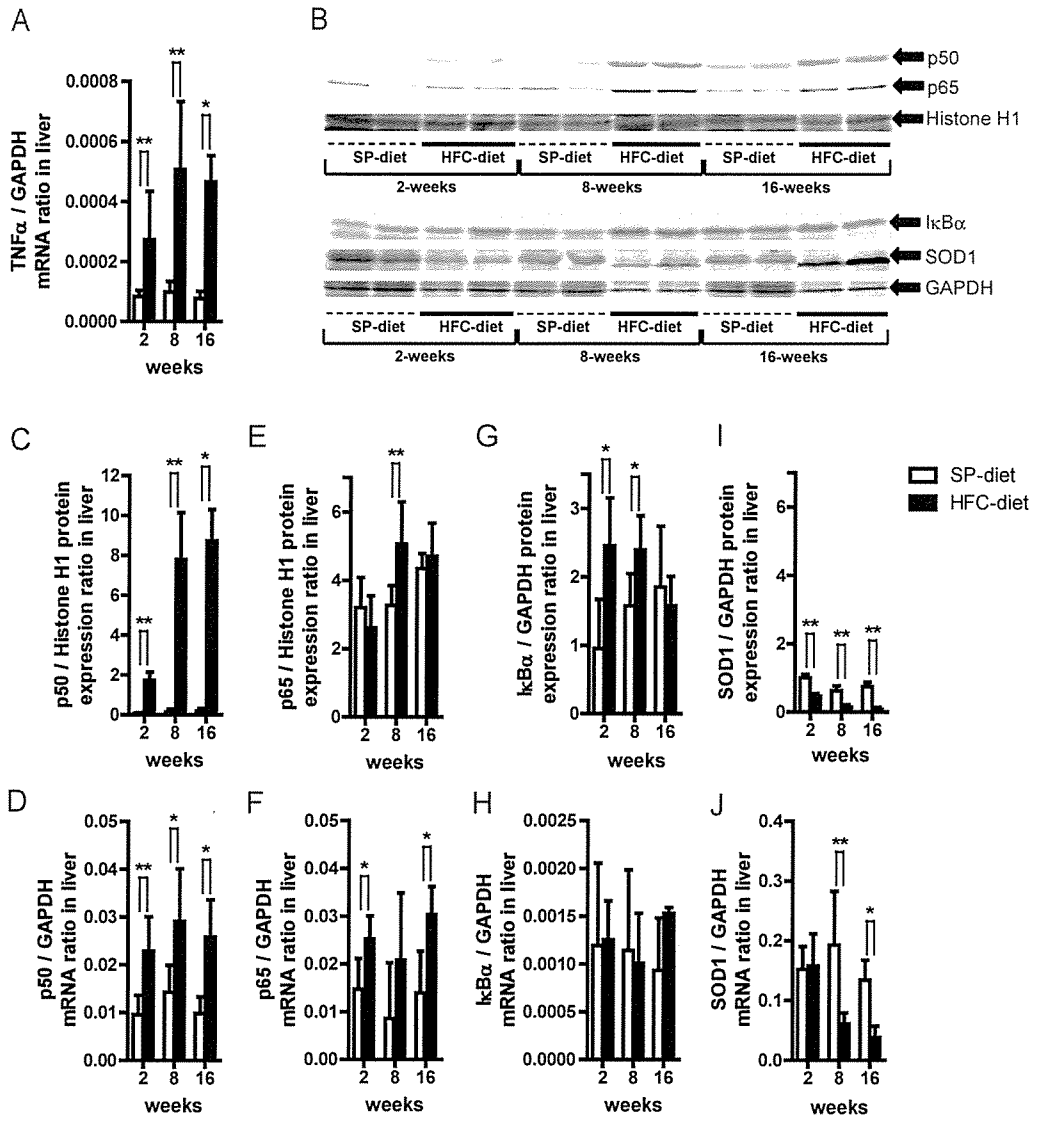
A
TNFα / GAPDH mRNA ratio in liver
0.0008
0.0006
0.0004
0.0002
0.0000
2 8 16
weeks
B
p50
p65
Histone H1
SP-diet HFC-diet SP-diet HFC-diet SP-diet HFC-diet
2-weeks 8-weeks 16-weeks
IκBα
SOD1
GAPDH
SP-diet HFC-diet SP-diet HFC-diet SP-diet HFC-diet
2-weeks 8-weeks 16-weeks
C
p50 / Histone H1 protein expression ratio in liver
E
p65 / Histone H1 protein expression ratio in liver
G
IκBα / GAPDH protein expression ratio in liver
I
SOD1 / GAPDH protein expression ratio in liver
SP-diet
HFC-diet
D
p50 / GAPDH mRNA ratio in liver
F
p65 / GAPDH mRNA ratio in liver
H
IκBα / GAPDH mRNA ratio in liver
J
SOD1 / GAPDH mRNA ratio in liver
weeks

Figure 1.

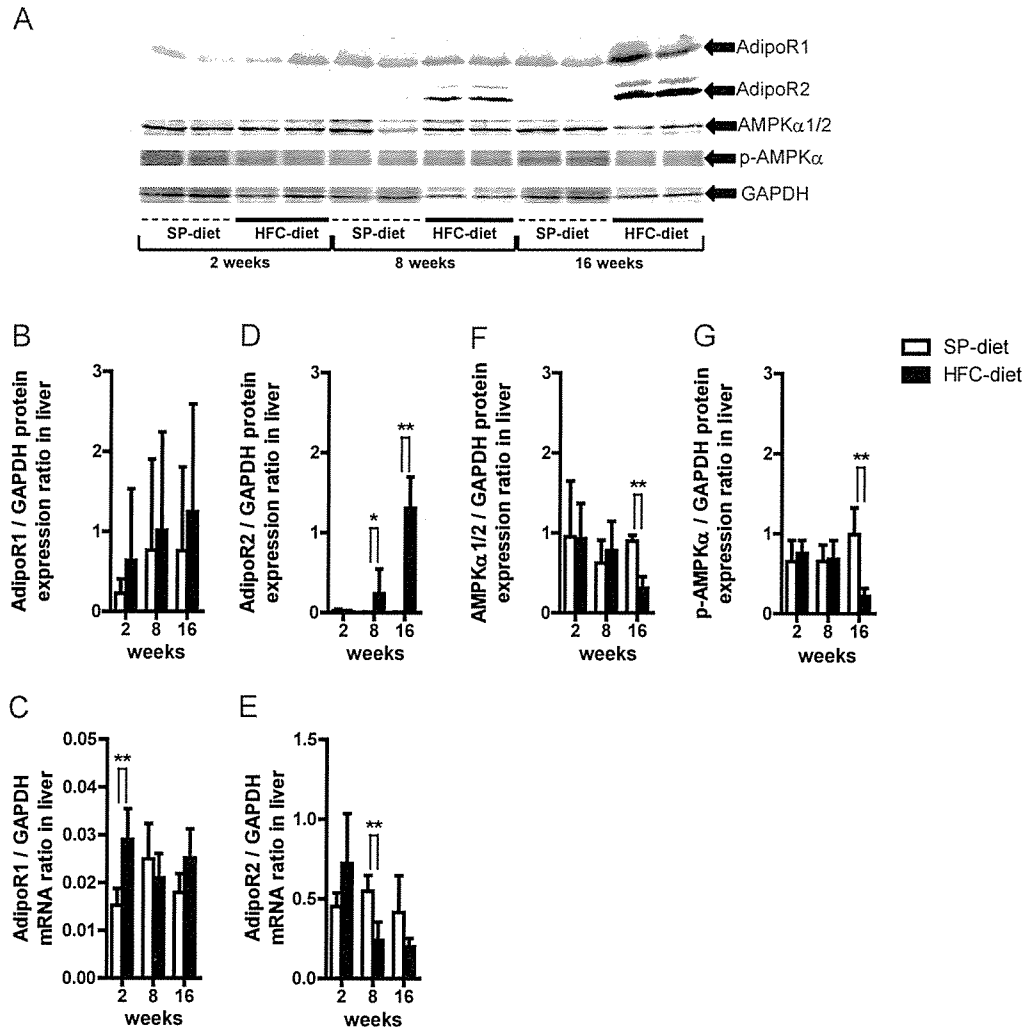
A
AdipoR1
AdipoR2
AMPKα1/2
p-AMPKα
GAPDH
SP-diet
HFC-diet
SP-diet
HFC-diet
SP-diet
HFC-diet
2 weeks
8 weeks
16 weeks
B
AdipoR1 / GAPDH protein expression ratio in liver
D
AdipoR2 / GAPDH protein expression ratio in liver
F
AMPKα1/2 / GAPDH protein expression ratio in liver
G
p-AMPKα / GAPDH protein expression ratio in liver
SP-diet
HFC-diet
weeks
C
AdipoR1 / GAPDH mRNA ratio in liver
E
AdipoR2 / GAPDH mRNA ratio in liver

Figure 2.

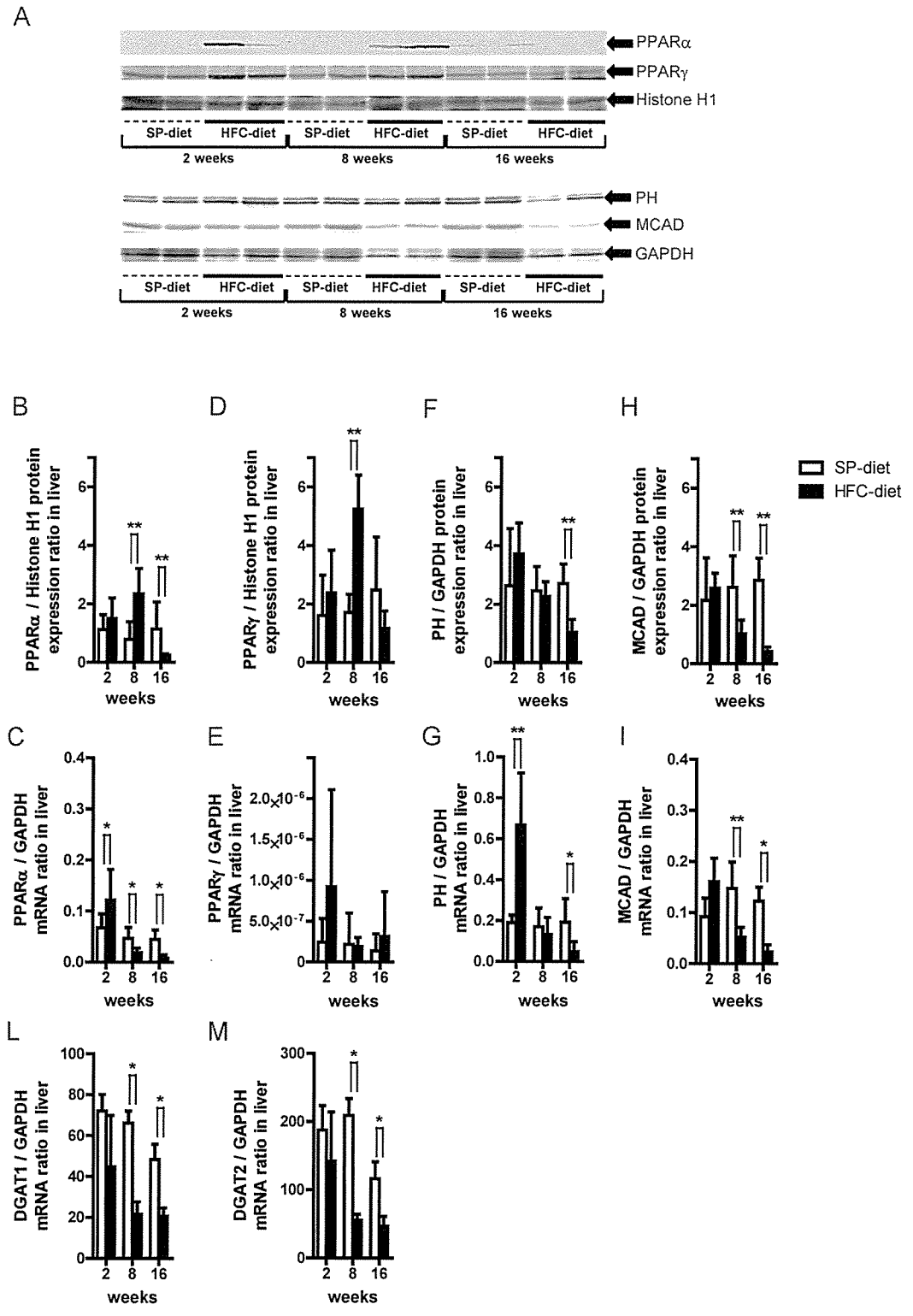
A
PPARα
PPARγ
Histone H1
SP-diet
HFC-diet
2 weeks
8 weeks
16 weeks
PH
MCAD
GAPDH
B
PPARα / Histone H1 protein expression ratio in liver
D
PPARγ / Histone H1 protein expression ratio in liver
F
PH / GAPDH protein expression ratio in liver
H
MCAD / GAPDH protein expression ratio in liver
C
PPARα / GAPDH mRNA ratio in liver
E
PPARγ / GAPDH mRNA ratio in liver
G
PH / GAPDH mRNA ratio in liver
I
MCAD / GAPDH mRNA ratio in liver
L
DGAT1 / GAPDH mRNA ratio in liver
M
DGAT2 / GAPDH mRNA ratio in liver
weeks

Figure 3.

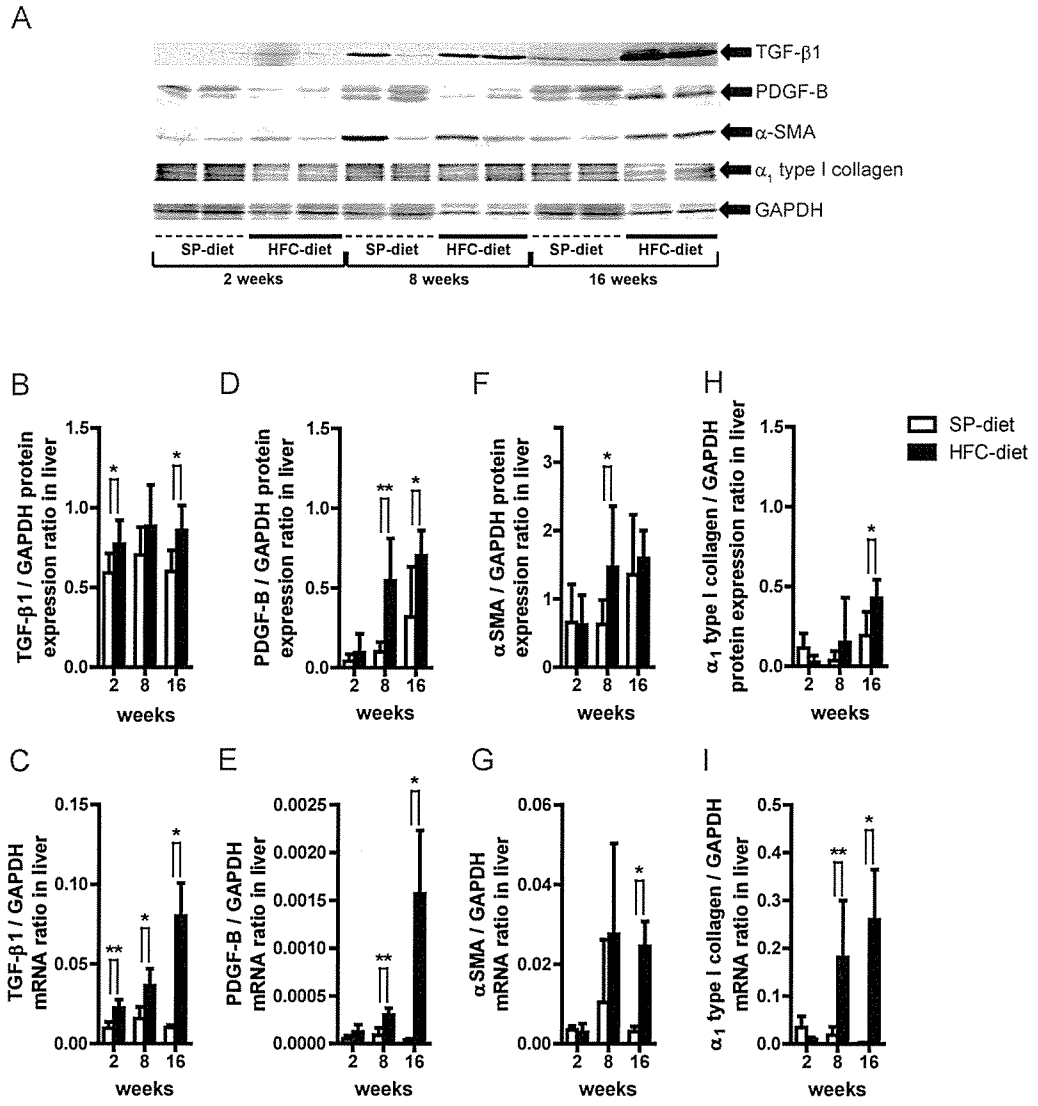
A
TGF-β1
PDGF-B
α-SMA
α1 type I collagen
GAPDH
SP-diet
HFC-diet
SP-diet
HFC-diet
SP-diet
HFC-diet
2 weeks
8 weeks
16 weeks
B
TGF-β1 / GAPDH protein expression ratio in liver
D
PDGF-B / GAPDH protein expression ratio in liver
F
αSMA / GAPDH protein expression ratio in liver
H
α1 type I collagen / GAPDH protein expression ratio in liver
SP-diet
HFC-diet
C
TGF-β1 / GAPDH mRNA ratio in liver
E
PDGF-B / GAPDH mRNA ratio in liver
G
αSMA / GAPDH mRNA ratio in liver
I
α1 type I collagen / GAPDH mRNA ratio in liver
weeks

Figure 4.

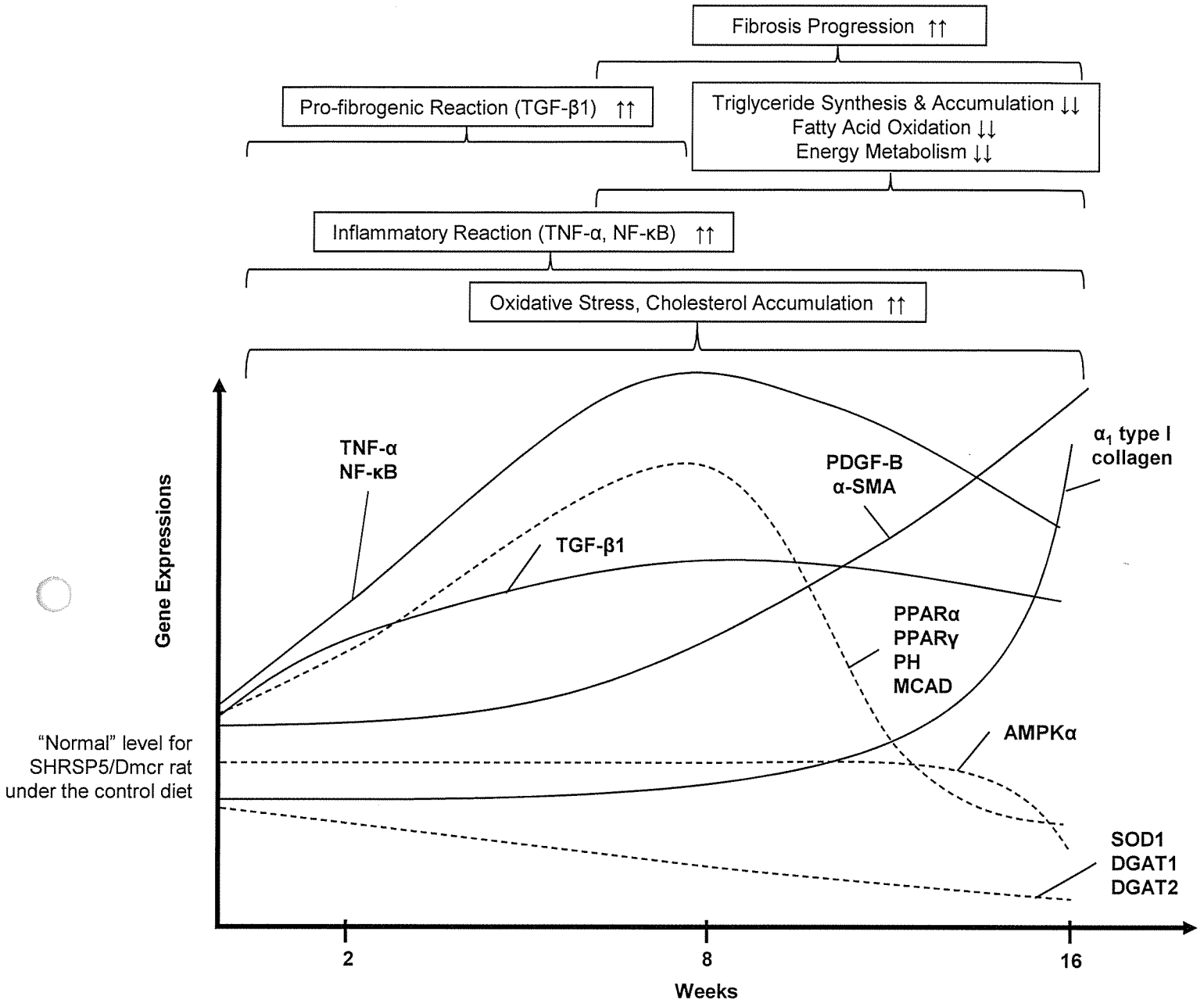
Fibrosis Progression ↑↑
Pro-fibrogenic Reaction (TGF-β1) ↑↑
Triglyceride Synthesis & Accumulation ↓↓
Fatty Acid Oxidation ↓↓
Energy Metabolism ↓↓
Inflammatory Reaction (TNF-α, NF-κB) ↑↑
Oxidative Stress, Cholesterol Accumulation ↑↑
Gene Expressions
TNF-α
NF-κB
TGF-β1
PDGF-B
α-SMA
α1 type I
collagen
PPARα
PPARγ
PH
MCAD
AMPKα
SOD1
DGAT1
DGAT2
"Normal" level for
SHRSP5/Dmcr rat
under the control diet
2
8
16
Weeks

Figure 5.